Catal Lett (2008) 125:201–208
DOI 10.1007/s10562-008-9592-4

Isotope Effects in Methanol Synthesis and the Reactivity of Copper Formates on a Cu/SiO_2 Catalyst

Y. Yang · C. A. Mims · R. S. Disselkamp · D. Mei · Ja-Hun Kwak · J. Szanyi · C. H. F. Peden · C. T. Campbell

Received: 2 May 2008 / Accepted: 15 July 2008 / Published online: 13 August 2008

Abstract Here we investigate isotope effects on the catalytic methanol synthesis reaction and the reactivity of copper-bound formate species in CO_2–H_2 atmospheres on Cu/SiO_2 catalysts by simultaneous IR and MS measurements, both steady-state and transient. Studies of isotopic variants (H/D, $^{12}C/^{13}C$) reveal that bidentate formate dominates the copper surface at steady state. The steady-state formate coverages of HCOO (in 6 bar 3:1 H_2:CO_2) and DCOO (in D_2:CO_2) are similar and the steady-state formate coverages in both systems decrease by $\sim$80% from 350 K to 550 K. Over the temperature range 413 K–553 K, the steady-state methanol synthesis rate shows a weak H/D isotope effect (1.05 ± 0.05) with somewhat higher activation energies in H_2:CO_2 (79 kJ/mole) than D_2:CO_2 (71 kJ/mole) over the range 473 K–553 K. The reverse water gas shift (RWGS) rates are higher than methanol synthesis and also shows a weak positive H/D isotope effect with higher activation energy for H_2/CO_2 than D_2/CO_2 (108 vs. and 102 kJ/mole) The reactivity of the resulting formate species in 6 bar H_2, 6 bar D_2 and 6 bar Ar is strongly dominated by decomposition back to CO_2 and H_2. H_2 and D_2 exposure compared to Ar do not enhance the formate decomposition rate. The decomposition profiles on the supported catalyst deviate from first order decay, indicating distributed surface reactivity. The average decomposition rates are similar to values previously reported on single crystals. The average activation energies for formate decomposition are 90 ± 17 kJ/mole for HCOO and 119 ± 11 kJ/mole for DCOO. By contrast to the catalytic reaction rates, the formate decomposition rate shows a strong H/D kinetic isotope effect (H/D $\sim$8 at 413 K), similar to previously observed values on Cu(110).

Keywords Isotope effects · Formate · Copper catalyst · Methanol synthesis · Reverse water gas shift · IR-MS

Y. Yang · R. S. Disselkamp · D. Mei · J.-H. Kwak · J. Szanyi · C. H. F. Peden
Institute for Interfacial Catalysis, Pacific Northwest National Laboratory, Richland, WA 99354, USA

C. A. Mims (✉)
Department of Chemical Engineering and Applied Chemistry, University of Toronto, 200 College Street, Toronto, Ontario, Canada M5S 3E5
e-mail: charles.mims@utoronto.ca

Present Address:
R. S. Disselkamp
Columbia Basin College, 2600 North 20th Avenue, Pasco, WA 99301, USA

C. T. Campbell
Department of Chemistry, University of Washington, Seattle, WA 98195, USA

1 Introduction

Generating clean hydrogen for fuel cells is a key component of a possible future transition to a so-called hydrogen economy. One such path forward is coal gasification followed by the water-gas shift (WGS) reaction, $CO + H_2O \rightarrow CO_2 + H_2$. On the other hand methanol synthesis, $CO_2 + 3H_2 \rightarrow MeOH + H_2O$, provides an attractive way to "store" hydrogen chemically for later recovery by steam reforming, $H_2O + MeOH \rightarrow CO_2 + 3H_2$ [1, 2]. During these transformations, the WGS reaction can occur simultaneously, affecting the hydrogen selectivity in these reactions [1, 3, 4]. Thus, the behavior of intermediates formed on transition metal surfaces upon H_2/CO_2 exposure and under reaction conditions is of high

interest. Substantial previous research has investigated these issues with copper, the basis of commercial Cu/ZnO methanol synthesis catalysts [5–10]. This work has included microkinetic modeling of the kinetics in order to aid in identifying the optimum catalysis conditions. Formates have been proposed by many investigators as key intermediates in these processes [1, 2, 5, 10–13]. Although these studies differ in detail, most models agree that formates are formed from H_2/CO_2 as surface intermediates and further surface reactions lead to products, CO/H_2O and/or methanol/H_2O. The process is represented by the following diagram.

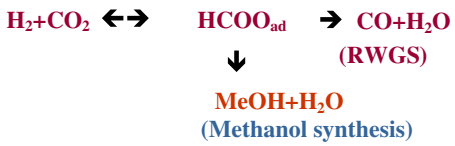

In this reaction network, the reactivity of formates with hydrogen is of particular interest. Some of the previous work has addressed formate reactivity on single crystal copper surfaces. For example, after exposure of a Cu (100) surface to a CO_2/H_2 mixture at 2.3 bar, it was observed that formates were synthesized and formed a stable coverage at temperatures below 363 K. These formates were removed upon exposure to 5.8 bar pure hydrogen in the same temperature range [11, 14]. However, no direct evidence can currently confirm that hydrogenation of surface formates leads to methanol product. Both experimental results [15] and theoretic simulations [2] indicate that hydrogen addition to formate is difficult. As a result, traditional surface analysis using elementary step by step investigations in ultra high vacuum can provide only limited information. Other studies have addressed surface formate reactivity on supported copper catalysts [16–18]. These studies have also observed the presence of surface-bound formate species under reaction conditions [16] and also have measured the stability of these species in inert gas and hydrogen [17, 18]. Compared with single crystal copper surfaces, the surface species observed on the oxide supported polycrystalline copper system are more complex because of the multi-faceted copper surfaces presented by the supported particles [14, 17, 19–21] and the presence of species adsorbed on the support materials (e.g., alumina and ceria) as well as the support-metal interface [22]. More complex infrared spectra are observed which makes assignment more difficult than on the single crystals [23–25]. A third factor is that the oxidation state of copper also affects the formation of surface species. Band shifts associated with the issues above are normally on the order of 20–40 cm^{-1} and bring confusion to vibrational mode assignments. For example, a 1,365 cm^{-1} peak has been either assigned as a bidentate formate C–H bending mode [26–28] or a monodentate formate O−C=O stretching mode [29–31]. Assignments of vibrational modes are assisted by investigation of isotopic variants; however, such experiments are currently absent from the literature. In addition, the catalytic rates of methanol synthesis and reverse water-gas shift (RWGS), as well as the reactivity of the bound formate species should exhibit H-D kinetic isotopic effects which could shed light on the reaction mechanism. To date, kinetic isotope effect measurements have not been reported for either methanol synthesis from CO_2:H_2 nor for formate reactivity on supported copper.

In this study we use a flow-through reactor system equipped with simultaneous in-situ, fast-scan transmission FTIR and mass spectrometric effluent analysis to study these effects on silica-supported copper catalysts under high pressure (6 bar) conditions. Isotopic variants (D_2/H_2, $^{12}C/^{13}C$) are used to (1) assign the major IR bands from surface-adsorbed species, particularly formates, and (2) measure H-D kinetic isotope effects of both the steady-state catalysis and the transient reactivity of the adsorbed formate species.

2 Experimental

The 10 wt.% Cu/SiO_2 catalyst employed in this study was prepared by incipient wetness impregnation using $Cu(NO_3)_2$ hydrate (Aldrich, 98 + % with low metal and salt impurities) and acid washed Davison 645 silica support material (stated BET area of 150 m^2/g). A silica support was chosen because previous IR studies have shown minimal support-bound species on silica and no evidence of copper metal-support interactions [16]. Prior to use, the catalyst was calcined in zero air overnight at 623 K, and then reduced within the reactor with pure H_2 (2.5 bar) at 553 K. XPS analysis of the catalyst before and after use revealed primarily Si, O, Cu features (>98%). The estimation of exposed copper surface sites was obtained by a standard N_2O titration method for polycrystalline copper [32, 33]. Typically, ~3.5 μmol (0.10 μmol/mg × 35.0 mg) of copper sites were present in any given sample.

The details of the transient kinetic analysis (TKA) reactor system have been described previously [34]. The reactor is loaded with ~35 mg catalyst of which ~4 mg are pressed onto a tungsten mesh centered in the optical path of a transmission FTIR spectrometer. The reactor itself is a made from a tungsten block heated by PID-controlled cartridge heaters (Watlow Inc.). The volume of the reaction zone is 0.5 cm^3 and can operate up to 10 bar total pressure over a temperature range of 150–770 K. Gas flow controllers (Alicat Scientific) and switching valves (VICI Valco Inc.) allow arbitrary choice of gas mixtures

with total flow rates from 1–200 sccm. The FTIR signal is obtained from a Bruker IFS/66S FTIR instrument equipped with a broadband MCT detector and fast (320 kHz) data acquisition electronics. Both the gas refresh rate in the reactor and FTIR scan rate are optimized in this way to achieve response times as low as ~1 s [34]. The MS can be switched to analyze either the reactor effluent or the inlet gas. Simultaneous control of and data acquisition from the IR and MS is by computer.

Both steady-state and transient experiments are employed. The steady-state catalytic turn-over frequencies (TOFs) are extracted from MS data, calibrated by analysis of known gas mixtures. The TOFs are obtained both at fixed temperatures and during a slow temperature ramping (2 K/min). The transient experiments involve initial exposure under constant gas exposure to a flowing gas mixture, followed by a switch to a different gas, keeping the same flow rate and pressure. The time resolved FTIR data are obtained from integrated intensities of specific adsorption features. FTIR background spectra were collected on the clean, freshly reduced catalyst at each temperature. In all experiments here, 10 sccm gas flow was used with pressures between 2.5 and 6.0 bar. Temperatures are explicitly given.

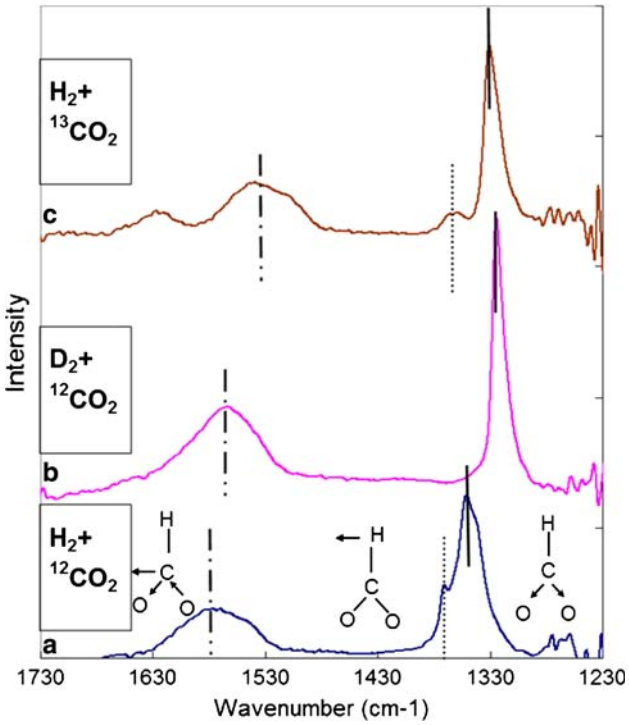

Fig. 1 Steady-state infrared spectra for a $H_2/^{12}CO_2$, b $D_2/^{12}CO_2$, and c $H_2/^{13}CO_2$ reagent gas feeds at 6 bar total pressure, hydrogen/carbon dioxide ratios = 3.0, T = 353 K. Solid vertical lines mark the symmetric O–C–O stretch, dashed lines the asymmetric O–C–O stretch and dotted lines, C–H bend. Note that the weaker 1,364 cm^{-1} mode remains relatively unchanged upon $^{12}CO_2/^{13}CO_2$ isotope substitution, and disappears on D substitution and therefore cannot be associated with a monodentate OCO stretching mode

3 Results and Discussion

3.1 Steady-State Experiments

3.1.1 FTIR Results at Steady State

Transmission infrared spectra of catalyst adsorbed species under steady-state reaction conditions are given in Fig. 1. The spectra were all taken at 393 K with input feedstreams consisting of (a) $H_2/^{12}CO_2$, (b) $D_2/^{12}CO_2$, and (c) $H_2/^{13}CO_2$ (all 3:1 molar ratio and 6 bar total pressure). Control experiments under these conditions on pure silica (not presented here) did not show any infrared spectral features in this region. In Fig. 1a, the 1,350 cm^{-1} band is relatively narrow (FWHM of ~30 cm^{-1}) with a less intense shoulder at ~1,365 cm^{-1} of comparable bandwidth. The 1,580 cm^{-1} band is much broader (FWHM estimated to be >60 cm^{-1}) and of much lower intensity. Under the conditions for Fig. 1a, we also observed (spectra not shown) two distinctive yet less intense peaks at 2,933 and 2,848 cm^{-1}. These have been previously assigned to adsorbed formate species [20, 21, 30]. The first is a combination band of asymmetric O–C=O stretch and C–H in-plane bend modes ($\nu_a(CO_2^-)+\delta$(C–H)), while the second arises from the C–H stretch modes. These high frequency features are often overlapped by other C–H modes [20, 35, 36] or support-bound species [23, 37] and, thus, are not as useful for monitoring copper adsorbate behavior.

The prominent band in $H_2/^{12}CO_2$ at 1,350 cm^{-1} is assigned to the O–C–O symmetric stretching mode ($\nu_s(CO_2^-)$) [10, 14, 17, 18, 20, 21, 38, 39], whereas the less intense, broad, 1,580 cm^{-1} mode is the corresponding asymmetric mode [20, 21, 26, 28, 29, 38], both referred to as bidentate formate on copper. Of particular interest is the weaker feature at 1,365 cm^{-1}. This feature has been variously assigned to (1) an O–C–O stretching vibration of a monodentate formate species [29, 31] or (2) to a C–H rocking mode (δ(C–H)) of bidentate formate [26–28]. The spectra for the isotopic variant experiments shown in Fig. 1b and c clearly favor the second interpretation. Noteably, it is found that this feature is removed upon H_2/D_2 isotope substitution (Fig. 1b) but remains relatively unchanged upon $^{12}CO_2/^{13}CO_2$ isotope substitution (Fig. 1c). This behavior is consistent with a C–H mode where the frequency depends on the mass of hydrogen atom and inconsistent with an O–C–O mode where the frequency depends on the mass of C–H group. The symmetric O–C–O stretch (1,350 cm^{-1} in Fig. 1a) is red shifted by a similar amount with either $^{12}C/^{13}C$ substitution (to 1,330 cm^{-1}) or H/D substitution (to 1,335 cm^{-1}) since

Table 1 Comparison of formate mode red shifts on $^{12}C/^{13}C$ isotope substitution

IR frequencies/Red shift			Assignment
This work	Bidentate formates on γ-alumina [40]		
	Experiment	Theoretic estimation [41]	
1,350 cm^{-1}/28 cm^{-1}	1,377 cm^{-1}/22 cm^{-1}	30 cm^{-1}	$\nu_s(CO_2^-)$
1,365 cm^{-1}/< 4 cm^{-1}	1,394 cm^{-1}/0 cm^{-1}	2 cm^{-1}	δ (CH)
1,580 cm^{-1}/40 cm^{-1}	1,597 cm^{-1}/43 cm^{-1}	37 cm^{-1}	$\nu_a(CO_2^-)$

the mass of the C–H group is increased by the same factor in both cases. The O–C–O asymmetric mode at 1,580 cm^{-1} is also red shifted by both $^{13}C/^{12}C$ and D/H substitution. The assignments here are consistent with previous $^{12}C/^{13}C$ isotope substitution studies of formate on alumina [40] and normal mode analysis [41]. This comparison is shown in Table 1.

Previous studies of formate coverage on Cu/SiO_2 versus temperature have been performed by Nakamura and coworkers [16–18] at one atmosphere pressure, wherein the coverages were quantified by desorption of CO_2 product after reaction. Here we extend measurements of formate coverage to 6 bar total pressure conditions in both $D_2/^{12}CO_2$ and $H_2/^{12}CO_2$ atmospheres. The integrated band intensities (normalized to those at 350 K) of the O–C–O symmetric stretch under steady-state conditions are shown as a function of reaction temperature in Fig. 2. No changes were observed in the appearances and central frequencies of the bands, but the intensities decrease by ~80% as the reaction temperature is increased 350 K to 550 K. This dependence is similar to that observed in reference [18] for HCOO. In addition, it is seen that both HCOO and DCOO behave essentially identically, thus indicating that the steady-state coverage of surface formate does not show an effect of H/D isotope substitution.

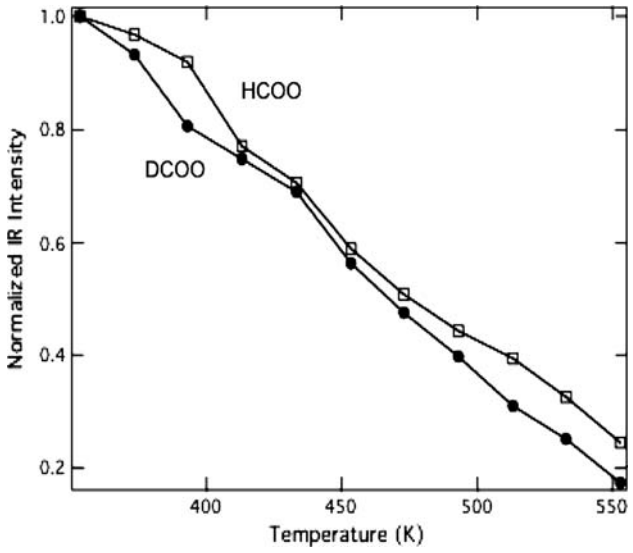

Fig. 2 Temperature dependence of formate ($\nu_s(CO_2^-)$) IR intensities at reaction steady state at 6 bar total pressure for HCOO in 3:1 H_2/CO_2 (open squares) and DCOO in 3:1 D_2/CO_2 (solid circles). Both HCOO and DCOO infrared intensities have been arbitrarily scaled to unity at the saturation values seen at 353 K

3.1.2 *Kinetics at Steady State*

Steady-state catalytic TOFs were measured for both the RWGS and methanol synthesis reactions in $H_2/^{12}CO_2$ and $D_2/^{12}CO_2$ (3:1) reagent gas feeds. Careful isothermal steady-state rate measurements were made at selected temperatures. In addition, the reaction rates were measured during a temperature programed sweep at 2 K/min. An initial set of measurements were made at 523 K and 553 K at 2.5 bar total pressure of 3:1 $H_2/^{12}CO_2$ to compare with previous reports on Cu/SiO_2 under these conditions [29]. These 2.5 bar results are shown in Table 2 along with results at 6 bar. The 2.5 bar values are within a factor of two of those reported previously [29], indicating similar catalytic behavior. Methanol synthesis rates show a strong pressure dependence, increasing by approximately a factor of 3 at 6 bar. The values in Table 2 at 523 K give a reaction order of 1.4 in total pressure which yields a TOF of around 4×10^{-3} s^{-1} when extrapolated to 42 bar total pressure. This value is consistent with methanol TOF measurements on Cu/SiO_2 tested under these industrial conditions [42]. By comparison the RWGS reaction rate is nearly zero-order in pressure.

The H/D kinetic isotope effects on the two reactions at 6 bar are shown in the Arrhenius plots of Fig. 3a and b. The upper curves (thinner line) are for H_2/CO_2 and lower curves (solid line) for D_2/CO_2 in both Fig. 3 panels. Panel (a) shows the CO product (RWGS) TOFs in both H_2/CO_2 and D_2/CO_2 reagent gas feed. Panel (b) shows a similar comparison for methanol synthesis. The isothermal points

Table 2 Turn-over frequencies (TOFs) are given for methanol synthesis and reverse water-gas shift products

TOF (s^{-1})	2.5 bar		6 bar	
	RWGS	MeOH	RWGS	MeOH
523 K	4.5×10^{-3}	7.2×10^{-5}	5.0×10^{-3}	2.5×10^{-4}
553 K	1.2×10^{-2}	1.6×10^{-4}	1.5×10^{-2}	4.5×10^{-4}

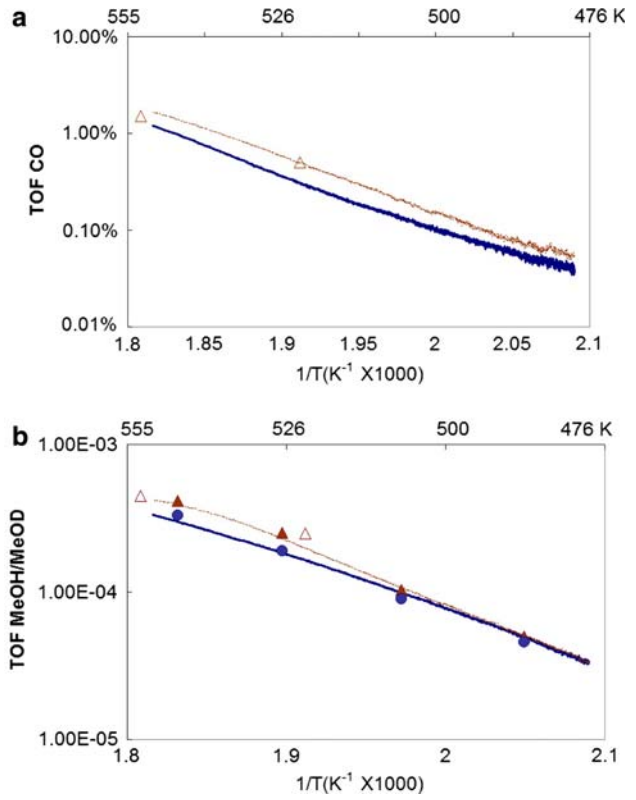

Fig. 3 Arrhenius plots of turn-over frequencies (TOFs) in units of molecule products per Cu site per second versus inverse temperature showing H/D kinetic isotope effects. Panel a data are for CO production (RWGS) and panel b data are for methanol synthesis. Feed gases are 3:1 $H_2(D_2)$:CO_2 at 6 bar total pressure. The solid lines are data measured in a temperature programed sweep, while the individual solid points are from bracketed isothermal experiments (see text). Additional open points data are from Table 2. In each panel, the upper lines and triangles are for the H variant, the lower lines and circles are for the D variant

from Table 2 are shown in both panels as open triangles for H_2/CO_2. In additional, the isothermal TOF points for methanol synthesis at each temperature (469, 488, 507, 527 and 546 K—solid data points) were obtained in a bracketed manner in single experiments. The H_2/CO_2 data (solid triangles) were measured, then the reactant gas was switched to obtain rates in D_2/CO_2 (solid circles), followed by a return to H_2/CO_2 to check for any activity changes. None were found. The raw temperature sweep MS intensity data were adjusted to fit the isothermal points and are shown by the solid lines in both Fig. 3a and b. At temperatures lower than shown in the figure (< 473 K), steady-state rates were not achieved during the temperature ramp due to slow time-to-steady state catalyst response, while at higher temperatures, methanol synthesis becomes limited by equilibrium yields. Fits of these results to the Arrhenius equation yield activation energies, E_a, for CO (Fig. 3a) production of 108 kJ/mole in H_2/CO_2 (upper, fine line) and a similar value of 102 kJ/mole in D_2/CO_2 (lower, solid line). E_a values for methanol synthesis were similar between D_2/CO_2 and H_2/CO_2 inputs but somewhat lower on average than E_a of CO. Slopes in the Arrhenius plots yield E_a values for methanol (Fig. 3b) production of 82 kJ/mole in H_2/CO_2 (upper, fine line) and a slightly lower value of 71 kJ/mole in D_2/CO_2 (lower, solid line). At higher temperature the curvatures are partially affected as the reaction reaches equilibrium. Another methanol (Fig. 3b) Arrhenius fit was applied to the steady state data points and yield very similar E_a values as 79 kJ/mole for H_2/CO_2 input (solid triangles) and 72 kJ/mole for D_2/CO_2 input (solid circles). The derived activation energy values in H_2/CO_2 are in good agreement with those reported previously for Cu(110) of 67 kJ/mole (methanol) [43] and from polycrystalline Cu where activation energy values of 77 kJ/mole (methanol) and 135 kJ/mole (CO) were seen [44]. A persistent H/D isotope effect (rate in H_2/rate in D_2) on CO production of approximately 1.5 is seen in the figure, while for methanol production the H/D isotope effect is 1.2 or less.

3.2 Titration Experiments

Figure 4 shows the decay of the DCOO ($\nu_s(CO_2^-)$) intensity when the adlayer, formed under D_2:CO_2 (3:1), is held in either D_2 (pink solid triangles) or Ar (blue solid circles)

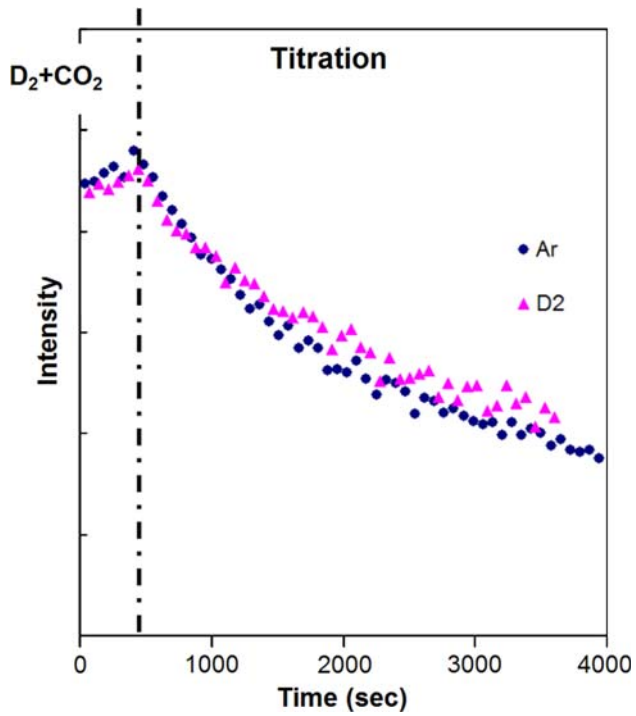

Fig. 4 D-formate IR (ν_S(OCO)) intensity decay versus time at 413 K. Adlayer was pre-formed in 3:1 D_2:CO_2 at 6 bar. A switch to 6 bar D_2 ((a), triangles) or 6 bar Ar ((b), circles). The time when the gases were switched is indicated as the dotted line

at 413 K and 6 bar gas pressure. Essentially identical decay profiles are observed for other IR modes. It is seen that the decay in D_2 is the same as in Ar. This general result is obtained at other temperatures and gas pressures for both DCOO formed in D_2:CO_2 and also for HCOO ($\nu_s(CO_2^-)$) adlayers formed in H_2/CO_2. These results indicate clearly that reduction in high pressure hydrogen/deuterium does not contribute significantly to the decay rate of bidentate copper formate on Cu/SiO_2. Previous results have indicated a significant role for a hydrogenation channel in the reaction of surface-adsorbed formate on Cu (100) [11], Cu [111], Cu [110] as well as Cu/SiO_2 catalysts [16–18], in contrast to the present results. The presence or absence of the hydrogen effect is discussed further below.

A large H/D kinetic isotope effect is observed in the formate disappearance and is shown in Fig. 5. Figure 5a shows the decay profiles in 6 bar Ar at 413 K for $HCOO^-$ (squares) and $DCOO^-$ (diamonds). $DCOO^-$ decays more slowly, with a characteristic time constant about 8 times as long as the $HCOO^-$, showing a positive H/D kinetic isotope effect (H faster than D). Decay kinetics were measured at 373, 393 and 413 K for HCOO while DCOO curves were obtained at 413, 423 and 433 K. The decomposition profiles are not well fit by first order decay kinetics, which we attribute to heterogeneous reactivity on the supported metal particles rather than non-unimolecular kinetics on a local scale. Figure 5 shows fits to the 413 K data based on a bi-exponential decay ($I/I_O = C_1 \exp(-t/J_1) + (1 - C_1) \exp(-t/J_2)$) where $C_1 = 0.4$ and J_1, $J_2 = 200$, 700 s for HCOO and 1,000, 7,500 s for DCOO. Similar fits are obtained for the rest of the data. Nevertheless, acceptable fits could be achieved with substantial latitude in the fit parameters and it was therefore not possible to assign reliable reactivity values or temperature trends from the behavior of the individual time constants. In light of these limitations, we represent the reactivity of the bound surface formates in these experiments by the reciprocal of the half-life of the formate adlayer given by the fits to the data. The temperature dependence of this reactivity value is shown in the Arrhenius plot in Fig. 5, panel b. From these plots, the derived Arrhenius expressions ($1/t_{1/2} = A_2 \exp\{-E_{A,2}/RT\}$) are $5.32 \times 10^{11} \exp\{(-119 \pm 11$ kJ/mole)/RT$\}$ for DCOO and $2.27 \times 10^8 \exp\{(-86 \pm 17$ kJ/mole)/RT$\}$ for HCOO. The H/D isotope effect from these analyses is 8 ± 3 at 413 K.

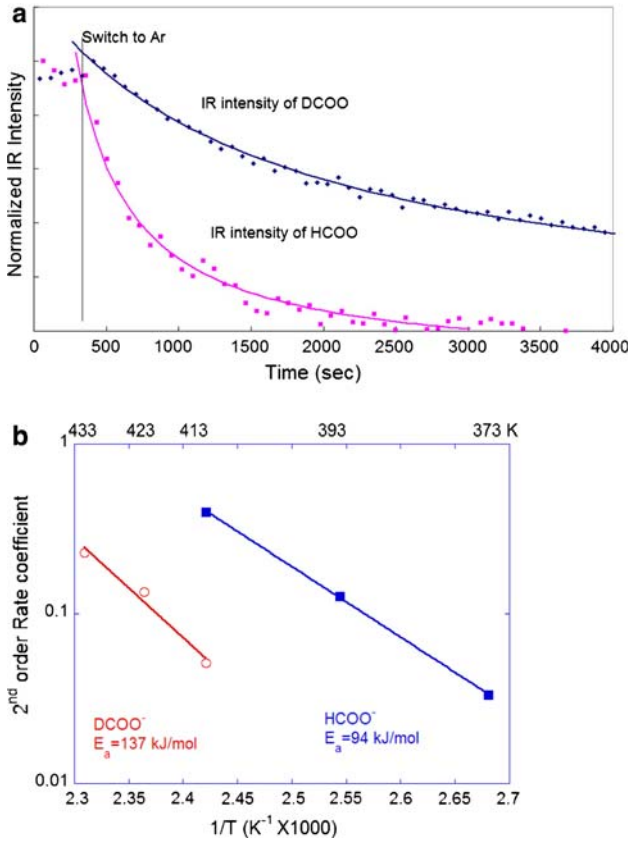

Fig. 5 Formate IR intesity decay versus time (panel a) in Ar (6 bar) at 413 K are shown for $HCOO^-$ (■) and $DCOO^-$ (◆). Fits to 2nd order kinetics are shown by the solid lines. Panel b shows Arrhenius plot of second order rate constants for HCOO decomposition (squares) and DCOO decomposition (circles)

4 General Discussion and Conclusions

4.1 Surface IR Assignments

The IR spectra of the isotopic variants confirmed that on reduced Cu/SiO_2 surfaces, bidentate formate is the only species observed under H_2/CO_2 atmospheres. The $\nu_s(CO_2^-)$ mode provides the best probe of surface formate coverage, and its narrow peak width provides excellent resolution of isotopomers for use in isotopic transient kinetics experiments. However, it is worth emphasizing here that the data presented were measured on freshly reduced catalysts. On an oxidized copper surface, the frequencies and intensities are altered from those on the reduced surface [17, 30, 31] generally interpreted as a shift to a monodentate surface structure. We observed similar changes in our studies after exposing the surfaces to oxygen, but did not observe any such changes to the IR spectra over periods of several hours at H_2/CO_2 exposed steady-state at various temperatures.

4.2 Formate Reactivity

The activation energies for formate decomposition on Cu(110) [45] are 136 kJ/mol (DCOO) and 133 kJ/mol (HCOO), similar to our nominal value for DCOO. Furthermore, our two time constant values overlap those

reported in reference [45].The reactivity of copper surface formates in hydrogen has been previously investigated. Chorkendorff, et al. [11], exposed formate adlayers on Cu (100) to hydrogen at 5.8 bar. The time constants of formate decay were observed to range from 300 to 3,000 s [46], similar to our rates but at substantially lower temperatures than ours ($\sim$40 K). The derived activation energy in the prior Chorkendorff study was 82 kJ/mole—close to our results for HCOO. Formate decay in this study was attributed by inference (products were not measured) to hydrogenation to methanol. Other studies by J. Nakamura and coworkers [16–18] examined formate reactivity in hydrogen atmospheres on Cu [111], Cu [110] and Cu/SiO_2. Their measured time constants on the Cu/SiO_2 surface agree well with ours at similar temperatures as does their activation energy (107.9 kJ/mole). Although they observed an effect of hydrogen pressure, no hydrogenation products were observed in their real time gas chromatograph (GC) record and they attributed the formate decay to decomposition back to CO_2 and H_2. In our titration experiments in hydrogen, the production of methanol was monitored and always accounted for less than 3% of the decomposed formate. This finding and the absence of a hydrogen effect on the formate decay rate at 6 bar strengthen the case for decomposition to CO_2 and H_2 as the major reaction channel under these conditions. We will publish more complete studies of the formate reaction channels in the near future.

The formate decomposition channel is shown here to have a strong H/D kinetic isotope effect, indicating involvement of H(D) in the decomposition mechanism. The kinetic isotope effect measured here is similar to the factor of 2.9–4.4 measured in TPD on Cu(110) in this temperature range [45]. It is close to the value of 6 predicted for a normal primary kinetic isotope effect for C–H bond cleavage at 413 K (due to the 5.5 kJ/mol larger zero-point vibrational energy for C–H versus C–D bonds [47] Single crystal studies of formate decomposition [12, 45] clearly show simple unimolecular (first order) decomposition kinetics, hence our conclusion that surface heterogeneity is responsible for the non-first order decays seen here. The difference in the average activation energies given by our data is higher than the expected difference in zero-point energies, but in view of the complexity of the kinetics, no significance is attached to this observation.

Despite the strong kinetic effect in the transient decay experiments, the steady-state catalytic reactions show very modest H/D kinetic isotope effects. The result that methanol synthesis is insensitive to H/D substitution makes it unlikely that a simple hydrogenation of surface formate is the rate-limiting step in methanol synthesis under these conditions. Though recent studies do not assume that formate is an intermediate in the RWGS channel leading to CO [48], the modest kinetic isotope effect seen here could result from a variety of elementary steps not related to the formate intermediate (such as surface O and H recombination) and therefore our results neither add nor detract from these arguments. We expect that these data, including the kinetic isotope effects will be useful in validation of microkinetic models.

Acknowledgments This project was performed at the *Institute for Interfacial Catalysis* (ICC) at Pacific Northwest National Laboratory (PNNL), and funded by a Laboratory Directed Research and Development (LDRD) grant as part of the Catalysis Initiative program administered by PNNL. The work was carried out in the Environmental Molecular Sciences Laboratory (EMSL) at PNNL, a National Scientific User facility supported by the US Department of Energy Office of Biological and Environmental Research. PNNL is operated by Battelle Memorial Institute for the U.S. Department of Energy. CTC would like to acknowledge the Department of Energy, Office of Basic Energy Sciences, Chemical Sciences Division grant number DE-FG02-96ER14630, for support of this work. CAM gratefully acknowledges PNNL support for his participation as visiting professor during the summer of 2007.

References

1. Chinchen GC, Denny PJ, Jennings JR, Spencer MS, Waugh KC (1988) Appl Catal 36:1
2. Askgaard TS, Nørskov JK, Ovesen CV, Stolze P (1995) J Catal 156:229
3. Fiolitakis E, Hofmann H (1983) J Catal 80:328
4. Choi Y, Stenger HG (2003) J Power Sources 124:432
5. Schumacher N, Boisen A, Dahl S, Gokhale AA, Kandoi S, Grabow LC, Dumesic JA, Mavrikakis M, Chorkendorff I (2005) J Catal 229:265
6. Ovesen CV, Stoltze P, Norskov JK, Campbell CT (1992) J Catal 134:445
7. Ernst K-H, Campbell CT, Moretti G (1992) J Catal 134:66
8. Avastuy JL, Gutierrez-Ortiz MA, Gonzalez-Marcos JA, Aranzabal A, Gonzalez-Velasco JR (2005) Ind Eng Chem Res 44(1):41
9. Kusar H, Hocevar S, Levec J (2006) Appl Catal B-Environ 63(3–4):194
10. Qi XM, Flytzani-Stephanopoulos M (2004) Ind Eng Chem Res 43(12):3055
11. Chorkendorff I, Taylor PA, Rasmussen PB (1992) J Vac Sci Technol A 10:2277
12. Wachs IE, Madix R (1978) J Catal 53:208
13. Russell JN Jr, Gates SM, Yates JT Jr (1985) Surf Sci 163:516
14. Taylor PA, Rusmussen PB, Ovesen CV, Stoltze P, Chorkendorff I (1992) Surf Sci 261:191
15. Nerlov J, Chorkendorff I (1999) J Catal 181:271
16. Yatsu T, Nishimura H, Fujitani T, Nakamura J (2000) J Catal 191:423
17. Nakano H, Nakamura I, Fujitani T, Nakamura J (2001) J Phys Chem B 105:1355
18. Nakamura I, Nakano H, Fijitani T, Uchijima T, Nakamura J (1999) J Vac Sci Technol A 17:1592
19. Sexton BA (1979) Surf Sci 88:319
20. Sexton BA, Hughes AE, Avery NR (1985) Surf Sci 155:366
21. Bowker M, Haq S, Holroyd R, Parlett PM, Poulston S, Richardson N (1996) J Chem Soc Faraday Trans 92:4683
22. Appel L, Eon JG, Schmal M (1998) Catal Lett 56:199

23. Goguet A, Meunier F, Breen JP, Burch R, Petch MI, Faur Ghenciu A (2004) J Catal 226:382
24. Meunier FC, Tibiletti D, Goguet A, Reid D, Burch R (2005) Appl Catal A: Gen 289:104
25. Meunier FC, Reid D, Goguet A, Shekhtman S, Hardacre C, Burch R, Deng W, Flytzani-Stephanopoulos M (2007) J Catal 247:277
26. Kuroda Y, Kubo M (1967) Spectrchimi Acta A 23:2779
27. Ito K, Bernstein H (1956) Can J Chem 34:170
28. Jones TS, Ashton R, Richardson NV (1989) J Chem Phys 90:7564
29. Clarke D, Lee D-K, Sandoval MJ, Bell AT (1994) J Catal 150:81
30. Millar GJ, Rochester CH, Waugh K (1991) J Chem Soc Faraday Trans 87:1491
31. Sakata Y, Domen K, Maruya K, Onishi T (1988–1989) Appl Surf Sci 35:363
32. Luys M-J, van Oeffelt PH, Pieters P, Ter Veen R (1991) Catal Today 10:283
33. Luys MJ, van Oeffelt PH, Brouwer WGJ, Pijpers AP, Scholten JJF (1989) Appl Catal 46:161
34. Yang Y, Disselkamp RS, Campbell CT, Szanyi J, Peden CHF, Goodwin JG Jr (2006) Rev Sci Instrum 77:094104
35. Millar GJ, Rochester CH, Waugh KC (1991) J Chem Soc Faraday Trans 87:2785
36. Millar GJ, Rochester CH, Waugh KC (1991) J Chem Soc Faraday Trans 87:2795
37. Denkwitz Y, Karpenko A, Plzak V, Leppelt R, Schumacher B, Behm RJ (2007) J Catal 246:74
38. Taylor PA, Rasmussen PB, Chorkendorff I (1991) J Phys Condens Matter 3:S59
39. Millar GJ, Rochester CH, Waugh KC (1992) Catal Lett 14:289
40. Greenler RG (1962) J Chem Phys 37:2094
41. Herzberg G (1945) Infrared and polyatomic molecules. D Van Nostrand Company, Inc., Princeton, p 169
42. Robbins JL, Iglesia E, Kelkar CP, DeRites B (1991) Catal Lett 10:1
43. Yoshihara J, Campbell CT (1996) J Catal 161:776
44. Yoshihara J, Campbell CT (1998) Surf Sci 407:256
45. Madix RJ, Telford SG (1992) Surf Sci 277:246
46. Taylor PA, Rasmussen PB, Chorkendorff I (1995) J Chem Soc Faraday Trans 91:1267
47. Gardiner WC (1972) Rates and mechanisms of chemical reactions. W.A. Benjamin, Inc., Menlo Park
48. Gokhale AA, James Dumesic A, Mavrikakis M (2008) J Amer Chem Soc 130:1402